

SPECIAL ISSUE PAPER

On downlink power allocation for multiuser variable-bit-rate video streaming

Yingsong Huang, Shiwen Mao* and Yihan Li

Department of Electrical and Computer Engineering, Auburn University, Auburn, AL 36849-5201, U.S.A.

ABSTRACT

In this paper, we study the problem of power allocation for streaming multiple variable-bit-rate (VBR) videos in the downlink of a cellular network. We consider a deterministic model for VBR video traffic and finite playout buffer at the mobile users. The objective is to derive the optimal downlink power allocation for the VBR video sessions, such that the video data can be delivered in a timely fashion without causing playout buffer overflow and underflow. The formulated problem is a nonlinear nonconvex optimization problem. We analyze the convexity conditions for the formulated problem and propose a two-step greedy approach to solve the problem. We also develop a distributed algorithm based on the dual decomposition technique, which can be incorporated into the two-step solution procedure. The performance of the proposed algorithms is validated with simulations using VBR video traces under realistic scenarios. Copyright © 2012 John Wiley & Sons, Ltd.

KEYWORDS

convex optimization; distributed algorithm; downlink power control; quality of service; multiuser video streaming; variable-bit-rate video

*Correspondence

Shiwen Mao, Department of Electrical and Computer Engineering, Auburn, University, Auburn, AL 36849–5201, U.S.A.

E-mail: smao@ieee.org

Part of this work was presented at ICST QShine 2010 [1].

1. INTRODUCTION

According to a recent study by Cisco, data traffic over wireless networks is expected to have a 26-fold increase over year 2010 by 2015 [2]. Furthermore, 66% of the increase in future wireless data traffic will be video related, as driven by the compelling need for ubiquitous access to mobile multimedia content for mobile users. Such drastic increase in video traffic will significantly stress the capacity of existing and future wireless networks. Considerable efforts are being made on developing new wireless network architectures and technologies to meet this *grand challenge*, such as video-aware ad hoc and mesh networks [3–5], wireless sensor networks [6–8], cognitive radio networks [9–12], femtocell networks [13,14], and cooperative relay networks [15,16]. Although new wireless architectures and technologies are being explored, it is also important to revisit existing wireless networks, to maximize their potential in carrying real-time video data.

In this paper, we consider the problem of streaming multiple user videos in the downlink of a cellular network. This is a highly relevant problem given the wide adoption and deployment of cellular networks for wireless access and the considerable amount of new

base stations (BSs) to be deployed every year.[†] Given the exploding wireless data and the quickly depleting spectrum resource, such cellular systems are usually interference limited. The capacity of a specific mobile user depends on the signal to interference-plus-noise ratio (SINR) at the user, which is a function of the power allocation for all the mobile users. Therefore, effective downlink power control is necessary for such a wireless video system to minimize the intracell interference for concurrent video sessions.

We consider the challenging problem of streaming multiuser variable-bit-rate (VBR) videos in the downlink of cellular networks. This is motivated by the fact that VBR video offers stable and superior quality over constant bit rate (CBR) videos. Furthermore, many stored video contents are coded in the VBR format. It is important to support such stored VBR video over existing wireless networks without the need for transcoding. The main challenge in supporting VBR video stems from its high rate variability and complex autocorrelation structure,

[†] It is reported that every year, 120,000 new base stations are added, catering to the 300–400 million new mobile phone users adopting mobile services around the world [17].

making it hard for network control and may cause frequent playout buffer underflow or overflow [18]. In this paper, we adopt a deterministic traffic model for stored VBR video, which jointly considers frame size, frame rate, and playout buffer size [19–21]. Unlike many existing work, we exploit effective downlink power control to adjust the downlink capacities for each VBR video session, on the basis of prior knowledge of frame sizes and playout buffer occupancies.

We present a downlink power control framework for streaming multiple VBR videos in a cellular network. With the deterministic VBR video traffic model, we formulate an optimization problem that jointly considers downlink power control, intracell interference, VBR video traffic characteristics, playout buffer underflow and overflow constraints, and BS peak power constraint. The objective is to maximize the total throughput, which can achieve high playout buffer utilization. As a result, playout buffer underflow or overflow events can be minimized. We analyze the convex/concave regions of the formulated problem and then develop a two-step downlink power allocation algorithm for solving the problem. We also derive a distributed algorithm based on the dual decomposition technique from convex optimization, to reduce the control and computation overhead at the BS. The performance of the proposed distributed algorithm is evaluated with simulations that use real VBR video traces. Our simulation results verify the accuracy of the analysis and demonstrate the efficacy of the proposed algorithms.

The remainder of this paper is organized as follows. The system model is presented in Section 2. We develop a two-step algorithm to solve the power allocation problem in Section 3, including a distributed power control algorithm based on dual decomposition in Section 3.3. Simulation results are presented in Section 4, and related work is discussed in Section 5. Section 6 concludes this paper. The notation used in this paper is summarized in Table I.

2. NETWORK AND VIDEO SYSTEM MODEL

We consider the downlink of a cellular network. In the cell, a BS streams multiple VBR videos simultaneously to mobile users in the cell, which share the common downlink bandwidth. We assume the last-hop wireless link is the bottleneck, whereas the wired segment of a session path is reliable with sufficient bandwidth [22]. As a result, the corresponding video data are always available at the BS before the scheduled transmission time.

Variable-bit-rate video traffic exhibits both strong asymptotic self-similarity and short-range correlation. A stochastic model capturing the complex autocorrelation structure often requires a large number of parameters and is thus hard to be incorporated for scheduling real-time video data. To this end, we adopt a *deterministic model*

Table I. Notation

Symbol	Description
N	Total number of users in a cell
L	Processing gain
β	Interference proportion
U	Set of users sharing the same channel
T_n	Total number of frames for user n video
b_n	Playout buffer size of user n
$D_n(t)$	Cumulative consumption curve at user n
$X_n(t)$	Cumulative transmission curve at user n
$B_n(t)$	Cumulative overflow curve at user i
$\bar{P}(t)$	BS transmit power vector in time slot t
\bar{P}_{\max}	Maximum power allocation vector without overflow
\bar{P}_{\min}	Minimum power allocation vector without underflow
\bar{P}	Peak power constraint for the base stations (BSs)
\bar{P}_{\min}	Sum of the elements in \bar{P}_{\min}
\bar{P}^*	Inflection power vector
\bar{P}	Optimal power vector
G_n	Path gain from BS to user n
B_{vw}	Channel bandwidth
τ	Duration of a time slot
η_n	Noise power at user n
C_n	Capacity from the BS to user n
B_{vw}	Channel bandwidth
κ	Constant for the proof of Lemma 2
$\bar{P}^i(t), \bar{P}^{ii}(t)$	Auxiliary power allocation in the Lemma 2 proof
A_n	Ratio of noise power and channel gain of user n
P_n^{th}	Minimum between P_n^{\max} and P_n^*
$\theta(l)$	Stepsize of step l in (32)
$\alpha_x(l), \alpha_n(l), \alpha_v(l)$	Stepsize of step l in (35)
$\gamma_n(t)$	Signal to interference-plus-noise ratio (SINR) at user un_n in time slot t
$\gamma_n^{\min}(t)$	Minimum SINR corresponding to $C_n^{\min}(t)$
$\gamma_n^{\max}(t)$	Maximum SINR for user un_n without overflow
γ_n^{th}	Receiver sensitivity at user n
F	$N \times N$ matrix defined in Equation (15)
λ, μ, ν	Lagrange multipliers
\mathcal{L}	Lagrange function

that considers frame sizes and playout buffers [20]. Let $D_n(t)$ denote the *cumulative consumption curve* of the n th mobile user, representing the total amount of bits consumed by the decoder from the beginning to time t . The cumulative consumption curve is determined by video characteristics such as frame sizes and frame rates. Assume that mobile user n has a playout buffer of size b_n bits and its video has T_n frames. We can derive a *cumulative overflow curve* for the user as

$$B_n(t) = \min\{D_n(t - 1) + b_n, D_n(T_n)\}, \forall t \quad (1)$$

$B_n(t)$ is the maximum number of bits that can be received at time t without overflowing user n 's playout buffer. Finally, we define *cumulative transmission curve* $X_n(t)$ as the cumulative amount of transmitted bits to user n from the beginning till time t . To simplify notation, we assume that the video sessions have identical frame rate and the frame intervals

are synchronized. Thus, a time slot t is equal to the t th frame interval, denoted as τ , for $0 \leq t \leq \max_n\{T_n\}$.[‡]

The three curves for user n are illustrated in Figure 1. A feasible transmission schedule will produce a cumulative transmission curve $X_n(t)$ that lies in between $D_n(t)$ and $B_n(t)$ (t), that is, causing neither underflow nor overflow at the playout buffer. In practice, $D_n(t)$ s are known for stored videos and can be delivered to the BS during session setup phase, and $B_n(t)$ s can be derived as in Equation (1) after the mobile users notify the BS of their playout buffer sizes.

We consider N subscribers in the cell, and let \mathcal{U} denote the set of mobile users sharing the downlink bandwidth. In each time slot t , the BS transmits to each user n with power $P_n(t)$, and the power allocation is denoted by a vector $\vec{P}(t) = [P_1(t), P_2(t), \dots, P_n(t)]^T$. We also consider a maximum transmit power constraint \bar{P} , that is, $\sum_{n \in \mathcal{U}} P_n(t) \leq \bar{P}$, for all t . When the power allocation $\vec{P}(t)$ is determined, the SINR at user n can be written as [23,24]

$$\gamma_n(\vec{P}(t)) = \frac{L_n G_n P_n(t)}{\beta \sum_{k \neq n} G_n P_k(t) + \eta_n} \quad (2)$$

where P_n is the power allocated to user n , G_n is the path gain between the BS and user n , η_n is the noise power at user n , L_n is a constant for user n (e.g., processing gain), and β denotes the orthogonality factor, with $0 \leq \beta \leq 1$. In this paper, we consider the case $\beta = 1$, where the SINR of a user depends on not only its own power allocation but also the power allocations of all other active users. Because the video frames have variable sizes and the video sessions have random phases, large frames from different sessions are less likely to occur in the same time slot. Jointly considering power allocation for the downlinks is, in some sense, analogous to statistical multiplexing of VBR video flows.

We assume slow-fading channels, where the path gains are random variables following certain distributions but do not change within each time slot [23]. The downlink capacity $C_n(t)$ depends on the SINR at user n , the channel bandwidth B_w , and the transceiver design, such as modulation and channel coding. Without loss of generality, we use the upper bound as predicted by Shannon's theorem for the downlink capacity:

$$C_n(\vec{P}(t)) = B_w \log\left(1 + \gamma_n(\vec{P}(t))\right) \quad (3)$$

[‡] If the frame rates are different, we can use a time slot duration that is equal to the greatest common divisor of all the frame intervals. If the frame intervals are not synchronized, a time slot can be a fraction of a frame interval within which the $D_n(t)$'s of all the videos remain constant. The problem formulation and proposed solution procedures to be discussed in the following sections still apply to these cases.

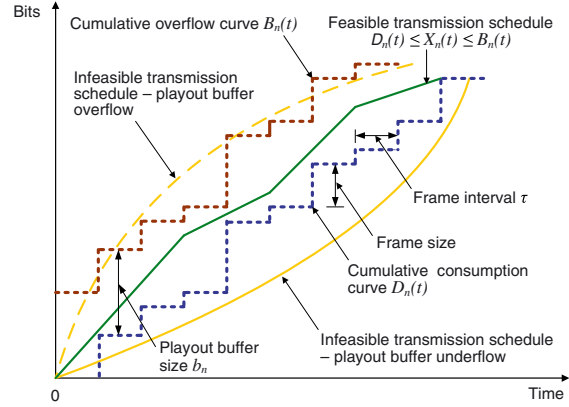


Figure 1. Transmission schedules for variable-bit-rate video session n .

In time slot t , $C_n(t)\tau$ bits of video data will be delivered to user n . The cumulative transmission curve $X_n(t)$ is

$$\begin{cases} X_n(0) = 0 \\ X_n(t) = X_n(t-1) + C_n(t)\tau, \quad \forall t \end{cases} \quad (4)$$

For a feasible power allocation, the cumulative transmission curves should satisfy

$$D_n(t) \leq X_n(t) \leq B_n(t), \quad \forall n, t \quad (5)$$

that is, without causing underflow or overflow at the playout buffer.

From Equations (3)~(5), the lower and upper limits on the feasible SINR at user n can be derived as

$$\gamma_n^{\min}(t) = \max\left\{ \exp\left\{ \frac{\max\{0, D_n(t) - X_n(t-1)\}}{B_w \tau} \right\}, \gamma_n^{\text{th}} \right\} \quad (6)$$

$$\gamma_n^{\max}(t) = \exp\left\{ \frac{B_n(t) - X_n(t-1)}{B_w \tau} \right\} \quad (7)$$

In Equation (6), γ_n^{th} is the minimum SINR requirement imposed by the transceiver design. The lower bound $\gamma_n^{\min}(t)$ in Equation (6) is the SINR that just empties the buffer at the end of time slot t , without causing underflow; the upper bound $\gamma_n^{\max}(t)$ in Equation (7) is the SINR that just fills up the buffer at the end of time slot t , without causing overflow.

Generally, the feasible power allocation $\vec{P}(t)$ is not unique for a given set of VBR video sessions. Among the set of feasible solutions, a schedule that transmits more data is more desirable because it provides more flexibility (i.e., a larger search space) for optimizing future power allocations. We formulate the problem of optimal downlink power control for VBR videos, termed Problem A, as

$$(A) \text{ maximize } \sum_{n \in \mathcal{U}} \log(1 + \gamma_n(t)) \quad (8)$$

subject to

$$\gamma_n(t) = \frac{L_n G_n P_n(t)}{\sum_{k \neq n} G_n P_k(t) + \eta_n}, \forall n \quad (9)$$

$$\gamma_n^{\min}(t) \leq \gamma_n(t) \leq \gamma_n^{\max}(t), \forall n \quad (10)$$

$$\sum_{n \in \mathcal{U}} P_n \leq \bar{P} \quad (11)$$

In Problem **A**, the objective is to achieve the maximum buffer utilization at the users, under playout buffer underflow and overflow constraints, and the BS maximum transmit power constraint. This is a nonlinear nonconvex problem, to which traditional convex optimization techniques cannot directly apply. Furthermore, because of the large variability of VBR traffic, the SINRs may assume values ranging from very low to very high, to avoid playout buffer underflow and overflow. Thus, the existing high SINR approximation [25] and low SINR approximation [26] techniques cannot be directly applied to solve this problem. We will analyze Problem (**A**) and obtain the optimality property in different power assignment region and develop an effective two-step solution procedure in the following sections.

3. TWO-STEP DOWNLINK POWER ALLOCATION

In Problem **A**, we consider an interference-limited system, where the capacity of mobile user n depends on the power allocations for all the active users. In the following, we first derive conditions for the optimal solution and then present a two-step power allocation algorithm for solving Problem **A**.

3.1. Properties

Lemma 1. *If there exists a feasible power allocation $\vec{P}(t)$ that achieves $\gamma_n^{\max}(t)$ for all user n , the solution is optimal.*

Proof. If the feasible power allocation $\vec{P}(t)$ achieves $\gamma_n^{\max}(t)$ for all user n , then all the user playout buffers will be full at the end of the time slot, according to Equation (6). Objective value (8) cannot be further improved without causing buffer overflow. Thus, the solution is optimal.

Lemma 2. *If the upper limit $\gamma_n^{\max}(t)$ cannot be achieved for every user n ; then, the optimal power allocation $\vec{P}(t)$ satisfies $\sum_{n \in \mathcal{U}} P_n(t) = \bar{P}$.*

Proof. Consider a feasible power allocation $\vec{P}'(t) = [P'_1(t), P'_2(t), \dots, P'_N(t)]^T$ that does not use all the BS power, that is, $\sum_{n \in \mathcal{U}} P'_n(t) < \bar{P}$. We can construct another feasible power allocation $\vec{P}''(t) = [P''_1(t), P''_2(t), \dots, P''_N(t)]^T$, such that $P''_n(t) = \kappa \cdot P'_n(t)$, for all n , and $\kappa \cdot \sum_{n \in \mathcal{U}} P'_n(t) =$

$\sum_{n \in \mathcal{U}} P''_n(t) \leq \bar{P}$, where $\kappa > 1$. For every user n , its SINR under the new power allocation is

$$\begin{aligned} \gamma_n(\vec{P}''(t)) &= \frac{L_n G_n P''_n(t)}{\sum_{k \neq n} G_n P''_k(t) + \eta_n} \\ &= \frac{\kappa L_n G_n P'_n(t)}{\sum_{k \neq n} \kappa G_n P'_k(t) + \eta_n} \\ &> \frac{\kappa L_n G_n P'_n(t)}{\sum_{k \neq n} \kappa G_n P'_k(t) + \kappa \eta_n} \\ &= \gamma_n(\vec{P}'(t)) \end{aligned}$$

The inequality is because $\kappa > 1$. It follows that $\sum_{n \in \mathcal{U}} \log(1 + \gamma_n(\vec{P}''(t))) > \sum_{n \in \mathcal{U}} \log(1 + \gamma_n(\vec{P}'(t)))$, because $\log(1+x)$ is an increasing function of x .

Furthermore, choosing $\kappa = \bar{P} / \sum_{n \in \mathcal{U}} P'_n(t)$, we can construct a feasible solution $\vec{P}'''(t) = \kappa \cdot \vec{P}'(t)$, such that $\sum_{n \in \mathcal{U}} P'''_n(t) = \bar{P}$. Then, we have $\gamma_n(\vec{P}'''(t)) > \gamma_n(\vec{P}'(t))$ and $\sum_{n \in \mathcal{U}} \log(1 + \gamma_n(\vec{P}'''(t))) > \sum_{n \in \mathcal{U}} \log(1 + \gamma_n(\vec{P}'(t)))$. That is, any feasible solution with $\sum_{n \in \mathcal{U}} P'_n(t) < \bar{P}$ will be dominated by feasible solutions with $\sum_{n \in \mathcal{U}} P'''_n(t) = \bar{P}$. We conclude that the optimal solution $\vec{P}(t)$ must satisfy $\sum_{n \in \mathcal{U}} P_n(t) = \bar{P}$.

We have the following result for the optimal solution of Problem **A**, which directly follows Lemmas 1 and 2.

Theorem 1. *A solution to Problem **A** is optimal if: (i) it achieves the maximum SINR $\gamma_n^{\max}(t)$ for all n ; or (ii) its total transmit power is \bar{P} .*

3.2. Two-step solution procedure

Theorem 1 implies that we can examine the SINR (or buffer) constraints and the peak power constraint separately. In the rest of this section, we present a two-step power allocation algorithm for solving Problem **A**. We first examine Problem **A** under condition (i) in Theorem 1, to obtain a simplified Problem **B** as

$$(B) \quad \gamma_n^{\max}(t) = \frac{L_n G_n P_n(t)}{\sum_{k \neq n} G_n P_k(t) + \eta_n}, \forall n \quad (12)$$

subject to

$$\sum_{n \in \mathcal{U}} P_n \leq \bar{P} \quad (13)$$

In Problem **B**, Equation (12) is a system of linear equations of power allocation $\vec{P}(t)$. Rearranging the terms, we can rewrite Equation (12) in the matrix form as

$$(\mathbf{I} - \mathbf{F})\vec{P}(t) = \vec{u}, \text{ for } \vec{P}(t) \succ \vec{0} \quad (14)$$

where \mathbf{I} is the identity matrix, \mathbf{F} is an $N \times N$ matrix with

$$F_{nm} = \begin{cases} 0, & \text{if } n = m \\ \gamma_n^{\max}/L_n, & \text{otherwise} \end{cases} \quad (15)$$

and $\vec{u} = [\eta_1\gamma_1^{\max}/L_nG_1, \eta_2\gamma_2^{\max}/L_nG_2, \dots, \eta_N\gamma_N^{\max}/L_nG_N]^T$.

Because all the variables are nonnegative, \mathbf{F} is a non-negative matrix. According to Perron–Frobenius theorem, we have the following equivalent statements [27]:

Fact 1. *The following statements are equivalent: (i) there exists a feasible power allocation satisfying Equation (14); (ii) the spectrum radius of \mathbf{F} is less than 1; (iii) the reciprocal matrix $(\mathbf{I} - \mathbf{F})^{-1} = \sum_{k=0}^{\infty} (\mathbf{F})^k$ exists and is component-wise positive.*

On the basis Theorem 1 and Fact 1, we derive the first step of the two-step power allocation algorithm, as given in Algorithm 1. If Problem **B** is solvable, the Step I algorithm in Algorithm 1 produces the optimal solution for Problem **A** according to Theorem 1. If Problem (**B**) is not

$$P_n^{\min}(t) \leq P_n(t) \leq P_n^{\max}(t), \forall n \quad (18)$$

$$\sum_{n \in \mathcal{U}} P_n(t) = \bar{P} \quad (19)$$

where $A_n = \eta_n/G_n > 0$ is the ratio of noise power and channel gain, representing the quality of the user n downlink channel. $P_n^{\min}(t)$ and $P_n^{\max}(t)$ are solved from Equations (10) and (17), as

$$P_n^{\min}(t) = \gamma_n^{\min} \cdot \frac{\bar{P} + A_n}{L_n + \gamma_n^{\min}} \quad (20)$$

$$P_n^{\max}(t) = \gamma_n^{\max} \cdot \frac{\bar{P} + A_n}{L_n + \gamma_n^{\max}} \quad (21)$$

Because the total transmit power is \bar{P} , the objective value in Equation (16) and the SINR in Equation (17) for each user only depends on its own power. Note that all the constraints are now linear. To solve Problem **C**, we examine the objective function to see if it is convex. We omit time index t in the following expressions for brevity.

Algorithm 1: Two-Step Power Allocation Algorithm: Step I

- 1 BS obtains b_n, D_n , and B_n , and computes γ_n^{\max} for all user n ;
 - 2 BS tests the existence of feasible solutions using (14);
 - 3 **if** (14) is solvable **then**
 - 4 | Compute its solution $\vec{P}(t)$;
 - 5 **else**
 - 6 | Go to Step II of the algorithm, as given in Algorithm 2;
 - 7 **end**
 - 8 **if** $\sum_{n \in \mathcal{U}} P_n(t) \leq \bar{P}$ **then**
 - 9 | Stop with the optimal solution $\vec{P}(t)$;
 - 10 **else**
 - 11 | Go to Step II of the algorithm, as given in Algorithm 2;
 - 12 **end**
-

feasible, we then derive Problem **C** by applying Lemma 2, as

$$(C) \text{ maximize } \sum_{n \in \mathcal{U}} \log(1 + \gamma_n(t)) \quad (16)$$

subject to

$$\gamma_n(t) = \frac{L_n P_n(t)}{\bar{P} - P_n(t) + A_n}, \forall n \quad (17)$$

Lemma 3. *The capacity of each user n , C_n has one inflection point P_n^* : when $P_n < P_n^*$, C_n is in concave; when $P_n > P_n^*$, C_n is convex.*

Proof. Taking the first and second derivatives of objective function (16) with respect to P_n , we have

$$\frac{\partial C_n(P_n)}{\partial P_n} = \frac{L_n(\bar{P} + A_n)}{(\bar{P} - P_n + A_n)[\bar{P} + (L_n - 1)P_n + A_n]} \quad (22)$$

$$\frac{\partial^2 C_n(P_n)}{\partial P_n^2} = \frac{-L_n[(L_n - 2)(\bar{P} + A_n) + 2(1 - L_n)P_n](\bar{P} + A_n)}{[(\bar{P} - P_n + A_n)^2 + L_n P_n(\bar{P} - P_n + A_n)]^2} \quad (23)$$

Because $P_n \leq \bar{P}$ and $A_n > 0$, both the first and second derivatives exist. Letting $\frac{\partial^2 C_n(P_n)}{\partial P_n^2} = 0$, we derive the unique inflection point

$$P_n^* = \frac{1}{2} \cdot \frac{L_n - 2}{L_n - 1} \cdot (\bar{P} + A_n) \quad (24)$$

When $P_n < P_n^*$, it can be shown that $\frac{\partial^2 C_n(P_n)}{\partial P_n^2} < 0$; when $P_n > P_n^*$, it can be shown that $\frac{\partial^2 C_n(P_n)}{\partial P_n^2} > 0$.

From Lemma 3, we can find the inflection point P_n^* that determines the convexity region of the objective capacity function. As an example, the normalized capacities for a two-user system are plotted in Figure 2, with the inflection points marked. It can be observed that the curves are concave on the left-hand side of the inflection points and convex on the right-hand side of the inflection points.

Usually the processing gain is large for practical systems (e.g., $L_n = 128$ in IS-95 CDMA). We assume $L_n \gg 1$ in the following analysis. Then, we have the following property for the solution to Problem C.

Theorem 2. For Problem C, there can be at most two links operating in the convex region if $L_n \geq (4\bar{P} + 6A_n)/(\bar{P} + 3A_n)$.

Proof. The reflection point is $P_n^* = \frac{1}{2} \cdot \frac{L_n - 2}{L_n - 1} \cdot (\bar{P} + A_n)$. As $L_n \rightarrow \infty$, we have $P_n^* = 0.5(\bar{P} + A_n) > 0.5\bar{P}$ because $A_n > 0$. Only one link can operate in the convex region because of peak power constraint (19) (i.e., no more than two powers can be larger than half of the peak power \bar{P}).

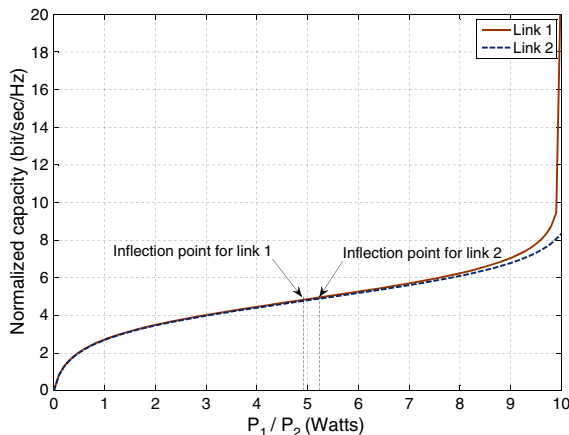


Figure 2. Normalized capacity curves and inflection points for a two-user system, where link 1 has better quality than link 2, that is, $A_1 < A_2$.

Because $\frac{\partial P_n^*}{\partial L_n} > 0$, P_n^* is an increasing function of L_n . When $1 \ll L_n < \infty$, we have $P_n^* < 0.5 \cdot (\bar{P} + A_n)$. Letting $3P_n^* = \bar{P}$, we have $L_n = (4\bar{P} + 6A_n)/(\bar{P} + 3A_n)$. Therefore if $L_n \geq (4\bar{P} + 6A_n)/(\bar{P} + 3A_n)$, only up to two users can have power allocation on the right-hand side of the inflection point, that is, the convex region.

For a clean channel where $A_n \approx 0$, $L_n \geq 4$ will guarantee at most two links operating in the convex region. The following results are on the impact of channel quality $A_n = \eta_n/G_n$.

Theorem 3. For a given L_n , the inflection point P_n^* is an increasing function of A_n . For two links i and j with the same transmit power P , if $A_i < A_j$, we have $C_i(P, A_i) > C_j(P, A_j)$ and $\frac{\partial C_i(P_i, A_i)}{\partial P_i} |_{P_i=P} > \frac{\partial C_j(P_j, A_j)}{\partial P_j} |_{P_j=P} > 0$.

Proof. The first part can be easily shown by the first derivative of P_n^* with respect to A_n , which is $\frac{\partial P_n^*}{\partial A_n} = \frac{L_n - 2}{2(L_n - 1)} > 0$, for $L_n > 2$. The second part can be easily shown by evaluating Equations (16), (17), and (22).

Theorem 3 shows that, for two links in the convex region with the same initial power P , allocating more power to the link with better quality can achieve a larger objective value than alternative ways of splitting the power between the two links (i.e., achieving the multiuser diversity gain). With the aforementioned analysis, we develop the *second step* of the power allocation algorithm for solving Problem C, as given in Algorithm 2. In Algorithm 2, Lines 4~7 test the feasibility of the power allocation. If the sum of the total minimum required power is larger than the BS peak power \bar{P} , there is no feasible power allocation and there will be buffer underflow. In this case, we select users with *good* channels for transmission and suspend the users with *bad* channels.

The Step II algorithm checks the three possible solution scenarios for Problem C depending on the network status and video parameters:

- All links operate in the concave region.
- One link operates in the convex region, and the remaining links operate in the concave region.
- Two links operate in the convex region, and the remaining links operate in the concave region.

Each of the three phases in Algorithm 2 checks the optimality condition for one of the three scenarios. In particular, Phase 1 first optimizes the power allocation in the concave region and then allocates the remaining power to the links that could be moved to the convex region. Phase 2 allocates as much power as possible to the link with the best quality, which could work in the convex region. Phase 3 attempts to move the second best link to the convex region if the total power constraint is not

violated. Usually when L_n and n are large, Phase 3 will rarely occur because of the peak power constraint.

In Algorithm 2, Line 11 presents a convex optimization component, for which several effective solution techniques can be applied. In the following section, we describe a distributed algorithm for Line 11 based on dual decomposition.

3.3. Distributed algorithm

As discussed in Section 3, the core of the Step II algorithm is to solve Problem C in the concave region (see Figure 2). In this section, we present a distributed algorithm for this purpose, where the mobile users are involved in power allocation to reduce the control and computation

Algorithm 2: Two-Step Power Allocation Algorithm: Step II

- 1 **Initialization**;
 - 2 BS obtains b_n , D_n , and B_n for all user n ;
 - 3 BS computes γ_n^{max} , γ_n^{min} , and P_n^* , for all n ;
 - 4 BS computes the minimum required sum power $\bar{P}_{min} = \sum_{n \in \mathcal{U}} P_n^{min}$ and gap $\Delta_P = \bar{P} - \bar{P}_{min}$;
 - 5 **if** $\bar{P}_{min} > \bar{P}$ **then**
 - 6 Remove links from \mathcal{U} , according to descending order of A_n , until $\bar{P}_{min} \leq \bar{P}$;
 - 7 **end**
 - 8 Compute $R_n = \frac{C_n(\min\{P_n^{max}, P_n^{min} + \Delta_P\}) - C_n(P_n^{min})}{\min\{P_n^{max}, P_n^{min} + \Delta_P\} - P_n^{min}}$, for all $P_n^{max} > P_n^*$;
 - 9 **Phase 1**;
 - 10 Select all the users satisfying $P_n^{min} < P_n^*$ as a set $\mathcal{U}' \subseteq \mathcal{U}$;
 - 11 Solve Problem C under constraints $P_n^{min} \leq P_n \leq \min(P_n^{max}, P_n^*)$ and $\sum_{n \in \mathcal{U}'} P_n \leq \bar{P}' = \bar{P} - \sum_{n \in \bar{\mathcal{U}}'} P_n^{min}$, where $\bar{\mathcal{U}}'$ is the complementary set of \mathcal{U}' , and obtain solution \bar{P}_1 ;
 - 12 Calculate R_n by updating P_n^{min} to the solution in Line 11 and assign the remaining power to the nodes in set \mathcal{U} , in descending order of R_n ;
 - 13 Obtain the Phase 1 solution, \bar{P}_{p_1} , and objective value f_{p_1} ;
 - 14 **Phase 2**;
 - 15 Select the link with the maximum R_n , and assign all the available power $\bar{P} - \bar{P}_{min}$ to the link, until either all the power is assigned or the link attains power P_n^{max} ;
 - 16 **if there is still power to allocate then**
 - 17 Select all the nodes in set $\mathcal{U} \setminus n$ and repeat Lines 8 ~ 12;
 - 18 **end**
 - 19 Obtain the Phase 2 solution, \bar{P}_{p_2} , and objective value f_{p_2} ;
 - 20 **Phase 3**;
 - 21 Select the first 2 links with the largest R_n 's, and assign all the available power $\bar{P} - \bar{P}_{min}$ to the links, until all the power is assigned or the links attains power P_n^{max} , and repeat Lines 16 ~ 18;
 - 22 Obtain the Phase 3 solution, \bar{P}_{p_3} , and objective value f_{p_3} ;
 - 23 **Decision**;
 - 24 Choose the largest objective value among f_{p_1} , f_{p_2} and f_{p_3} , and stop with the corresponding power assignment;
-

overhead on the BS. In the concave region, we have Problem **D** as

$$(D) \text{ maximize } \sum_{n \in \mathcal{U}} \log(1 + \gamma_n(t)) \quad (25)$$

subject to

$$\gamma_n(t) = \frac{L_n P_n(t)}{\bar{P} - P_n(t) + A_n}, \forall n \quad (26)$$

$$P_n^{\min}(t) \leq P_n(t) \leq \min\{P_n^{\max}, P_n^*\}, \forall n \quad (27)$$

$$\sum_{n \in \mathcal{U}} P_n(t) \leq P_{\text{tot}} \quad (28)$$

where $P_{\text{tot}} \leq \bar{P}$ is the total power budget for the links in the concave region, P_n^{\min} is given in Equation (20), and P_n^{\max} is given in Equation (21). For brevity, we define $P_n^{\text{th}} = \min\{P_n^{\max}, P_n^*\}$ and drop the time slot index t in the following analysis for brevity.

Introducing nonnegative Lagrange multipliers λ_n, μ_n , and ν for constraints (27) and (28), respectively, we obtain the Lagrange function as

$$\hat{P}_n(\hat{\lambda}_n, \hat{\mu}_n, \hat{\nu}) = \arg \max_{P_n^{\min} \leq P_n \leq P_n^{\text{th}}} \mathcal{L}_n(P_n, \hat{\lambda}_n, \hat{\mu}_n, \hat{\nu}), \forall n \quad (31)$$

Subproblem (31) has a unique optimal solution due to the strict concavity of \mathcal{L}_n . We use the gradient method [28] to solve (31), where user n iteratively updates its power P_n as

$$\begin{aligned} P_n(l+1) &= [P_n(l) + \theta(l) \nabla_n \mathcal{L}_n(P_n)]^* \\ &= [P_n(l) + \theta(l)(\lambda_n - \mu_n - \nu) + \end{aligned} \quad (32)$$

$$\theta(l) \frac{L_n(\bar{P} + A_n)}{(\bar{P} - P_n + A_n)(\bar{P} + (L_n - 1)P_n + A_n)}]^*$$

where $[\cdot]^*$ denotes the projection onto the range of $[P_n^{\min}, P_n^{\text{th}}]$. The update stepsize $\theta(l)$ varies in each step l and is determined by the Armijo rule [28]. Because of the strict concavity of \mathcal{L}_n , the series $\{P_n(1), P_n(2), \dots\}$ will converge to the optimal solution \hat{P}_n as $l \rightarrow \infty$.

Algorithm 3: Distributed Power Control Algorithm

- 1 BS sets $l = 0$ and prices $\lambda_n(l), \mu_n(l), \nu(l)$ equal to some nonnegative initial values for all n ;
 - 2 BS broadcasts the prices to the selected users;
 - 3 Each user locally solves problem (31) as in (32) to obtain its requested power;
 - 4 Each user sends its requested power to the BS;
 - 5 BS updates prices $\lambda_n(l), \mu_n(l), \nu(l)$ as in (35) and broadcasts new prices $\lambda_n(l+1), \mu_n(l+1), \nu(l+1)$ for all n ;
 - 6 Set $l = l + 1$ and go to Step 3, until the solution converges;
-

$$\begin{aligned} &\mathcal{L}(\vec{P}, \vec{\lambda}, \vec{\mu}, \nu) \\ &= \sum_{n \in \mathcal{U}} \left[\log \left(1 + \frac{L_n P_n}{\bar{P} - P_n + A_n} \right) + \lambda_n (P_n - P_n^{\min}) \right] + \\ &\quad \sum_{n \in \mathcal{U}} [\mu_n (P_n^{\text{th}} - P_n)] + \nu (P_{\text{tot}} - \sum_{n \in \mathcal{U}} P_n) \\ &= \sum_{n \in \mathcal{U}} [\mathcal{L}_n(P_n, \lambda_n, \mu_n, \nu) + (\mu_n P_n^{\text{th}} - \lambda_n P_n^{\min})] + \nu P_{\text{tot}} \end{aligned} \quad (29)$$

where

$$\mathcal{L}(P_n, \lambda_n, \mu_n, \nu) = \log \left(1 + \frac{L_n P_n}{\bar{P} - P_n + A_n} \right) + (\lambda_n - \mu_n - \nu) P_n \quad (30)$$

Because \mathcal{L}_n only depends on user n 's own parameters, we have the dual decomposition for each user n . For given Lagrange multipliers (or prices) $\hat{\lambda}_n, \hat{\mu}_n$, and $\hat{\nu}$, we have the following subproblem for each user n .

For a given optimal solution for problem (31), $\vec{\hat{P}} = [\hat{P}_1, \dots, \hat{P}_N]^T$, the master dual problem is as follows:

$$\text{minimize } \mathcal{L}(\vec{\hat{P}}, \vec{\lambda}, \vec{\mu}, \nu) \quad (33)$$

$$\text{subject to } \lambda_n, \mu_n, \nu \geq 0, \forall n \quad (34)$$

Because objective function (33) is differentiable, we also apply the gradient method to solve the master dual problem [28], where the Lagrange multipliers are iteratively updated as

$$\begin{cases} \lambda_n(l+1) = \left[\lambda_n(l) - \alpha_\lambda(l) \cdot \frac{\partial \mathcal{L}(\vec{\lambda}, \vec{\mu}, \nu)}{\partial \lambda_n} \right]^+, \forall n \\ \mu_n(l+1) = \left[\mu_n(l) - \alpha_\mu(l) \cdot \frac{\partial \mathcal{L}(\vec{\lambda}, \vec{\mu}, \nu)}{\partial \mu_n} \right]^+, \forall n \\ \nu(l+1) = \left[\nu(l) - \alpha_\nu(l) \cdot \frac{\partial \mathcal{L}(\vec{\lambda}, \vec{\mu}, \nu)}{\partial \nu} \right]^+ \end{cases} \quad (35)$$

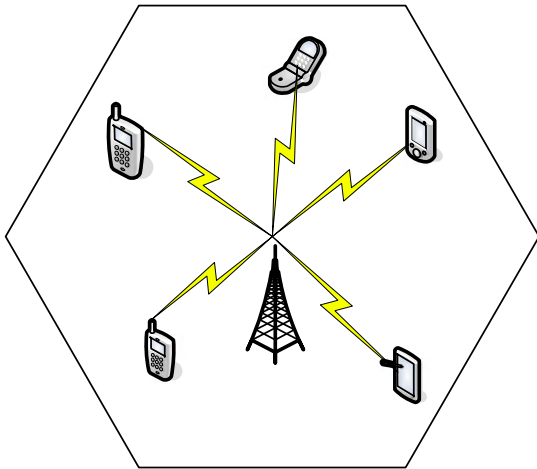


Figure 3. Topology of the cellular network.

where $[\cdot]^+$ denotes the projection onto the nonnegative axis. The update stepsizes are also determined by the Armijo rule [28]. As the dual variables $\vec{\lambda}(l), \vec{\mu}(l), v(l)$ converge to their stable values as $l \rightarrow \infty$, the primal variables \vec{P} will also converge to the optimal solution [29].

The distributed algorithm is given in Algorithm 3 where the aforementioned procedures are repeated iteratively. The BS first broadcasts Lagrange multipliers to the users. Each user updates its requested power as in Equation (32), using local information $P_n^{\min}, P_n^{\max}, P_n^*, A_n, L_n$, and BS peak power \bar{P} . Each user then sends its requested power back to the BS, and the BS will update the Lagrange multipliers as in Equation (35), and so forth, until the optimal solution is obtained.

4. SIMULATION STUDY

We evaluate the proposed algorithms with MATLAB simulations, where the deterministic VBR traffic model and the optimization solution algorithms are implemented. We use a cellular network with 20 users[§]; the network topology is illustrated in Figure 3. The downlink bandwidth is 1 MHz. The path gain averages are $G_n = d_n^{-4}$, where d_n is the physical distance from the BS to user n . The downlink channel is modeled as log-normal block fading with zero mean and variance 8 dB [23]. The processing gains are set to $L_n = 128$ for all n . The distance d_n is uniformly distributed in (100 m, 1000 m). The device temperature is $T_0 = 290$ K and the equivalent noise bandwidth is $B_w = 1$ MHz. The BS peak power constraints are set to $\bar{P} = 10$ Watts. We use three VBR movies traces, *Star Wars*,

[§] The number of users/links in the cellular network is chosen according to the resource specified in the simulation: bandwidth and the total BS power limit.

NBC News, and *Tokyo Olympics*, from the Video Trace Library maintained at Arizona State University [30]. We plot the sizes of the first 100 frames of the *NBC News* video sequence in Figure 4, to illustrate the high variation of VBR video frame sizes, which makes it very challenging to develop accurate mathematical models. Each playout buffer is set to 1.5 times of the largest frame size in the requested VBR video.

In the simulations, we have seven user streaming *NBC News*, seven users streaming *Star Wars*, and six users streaming *Tokyo Olympics*. The proposed power allocation algorithm is executed at the beginning of each time slot. In Figure 5, we plot the cumulative consumption, overflow, and transmission curves for *NBC News* transmitted to user 2. The top subfigure is the overview of 10,000 frames. We also plot the curves from frame 2620 to 2640 in the bottom subfigure. We observe that the cumulative transmission curve $X(t)$ is very close to the cumulative overflow curve $B(t)$, indicating that the algorithm always aim to maximize the transmission rate as allowed by the buffer and power constraints. The playout buffers are almost fully utilized most of the time. There is no playout buffer overflow and underflow for the entire range of 10,000 frames. Among the *NBC News* frames, frame 2625 is the largest frame. We let seven out of the 20 links playout this largest frame simultaneously at time slot 2625 in the simulation. There is no buffer underflow under such heavy load.

In Figure 6, we plot the power allocation and price updates for all the 20 links in one of the 10,000 time slots. The power and prices converge in around 70 steps. The converged power vector is $\vec{P} = [0.0022, 1.396, 0.0356, 0.0024, 1.396, 0.0351, 0.0016, 1.396, 0.0356, 0.0026, 1.396, 0.0356, 0.0023, 1.396, 0.0356, 0.0018, 1.396, 0.0356, 0.0034, 1.394]$ Watts. Note that with the distributed algorithm, the computation in each iteration is only consisting updating power or price as in Equations (32) and (35), which takes only a negligible amount of time. The 70-step convergence time is very small compared with

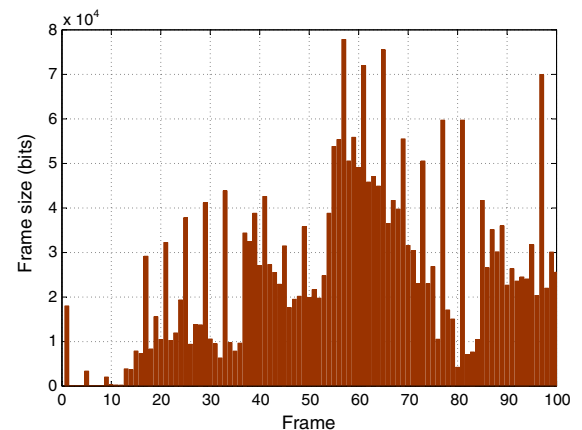


Figure 4. The sizes of the first 100 frames of the *NBC News* sequence.

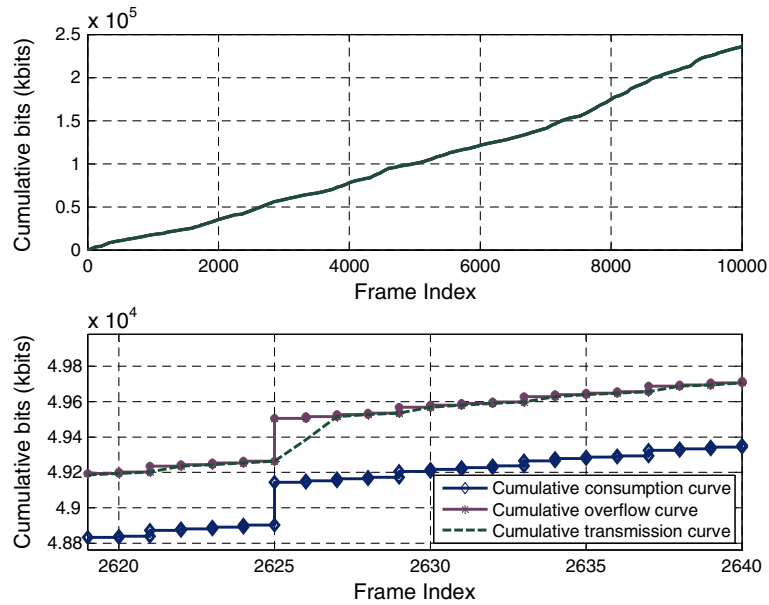


Figure 5. Transmission schedule for video *NBC News* to user 2.

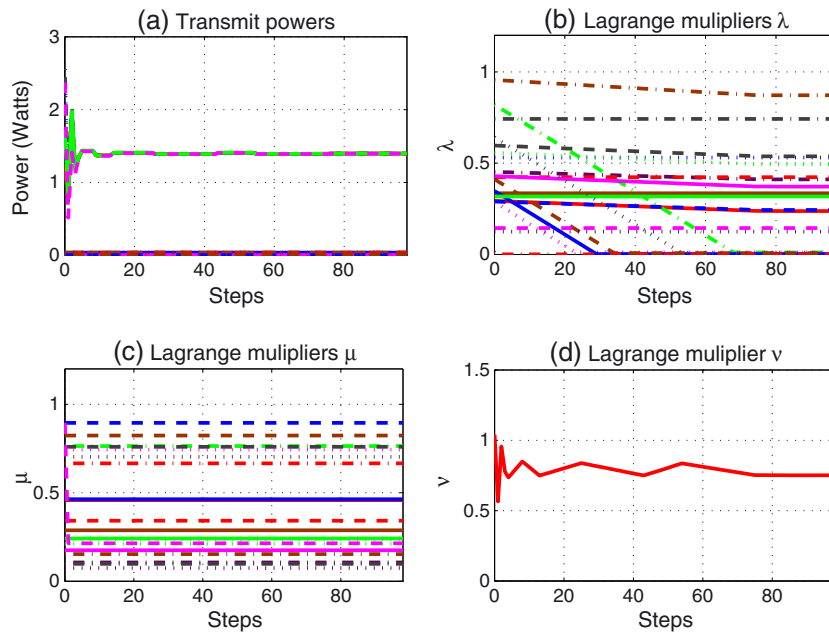


Figure 6. Convergence of power allocation and Lagrange multipliers.

the power control in cellular standards (e.g., 1500 Hz for UMTS power control [31]). Because the gradient method is used, the convergence of the algorithm is dependent on the gradients, which further depend on the system parameters such as L_n and A_n . Another main factor for the convergence speed is the choice of the stepsize. As discussed, we use Armijo rule to determine step size, in which the stepsize evolves according to the difference of the target values between steps.

Finally, we compare the proposed algorithm with a diversity-aware power allocation scheme, where the BS allocates power according to channel quality. With this scheme, the best channel n will be assigned power to achieve its maximum required power $P_n^{\max}(t)$. Then, the second best channel will be allocated power until its maximum required power is achieved, and so forth until all of \bar{P} is allocated. In this simulation, we increase the number of users to 50 to stress the capacity of the

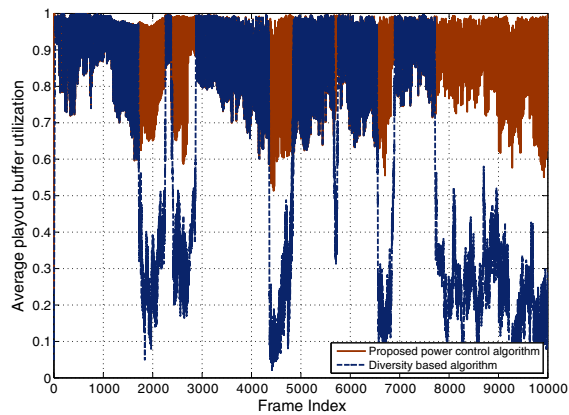


Figure 7. Average playout buffer utilization for the entire video sequence (10,000 frames).

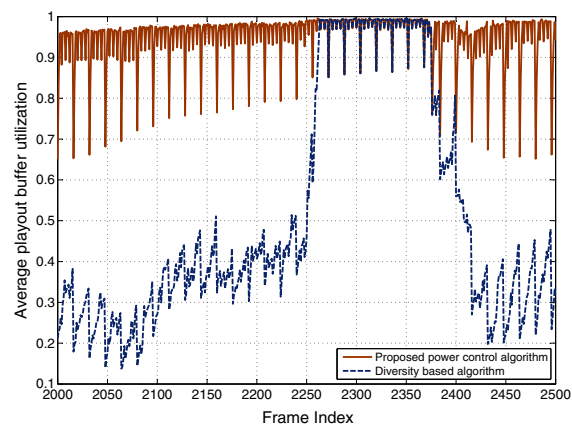


Figure 8. Average playout buffer utilization from frames 2000 to 2500.

cellular network, such that the system is close to saturate. The purpose is to show the performance of the algorithms under a nearly congested scenario, which is more interesting in performance analysis than an underload scenario.

We compare the algorithms by their average playout buffer utilization. In Figure 7, we plot the average buffer utilizations achieved by the proposed scheme and the diversity-aware scheme for the entire video sequence. A zoomed inversion is presented in Figure 8 from frames ranging from 2000 to 2500. It can be seen that the proposed algorithm consistently achieves high buffer utilization, ranging from 60% to 100%. The diversity scheme achieves buffer utilization lower than 50% for frames from 2000 to 2250. Such considerably higher buffer utilization translates to better video quality: there is no buffer overflow or underflow for proposed algorithm, whereas there is buffer underflow in 17% of the playout frames for the diversity scheme.

5. RELATED WORK

There have been several papers on VBR video over wired network. Because long-range-dependent VBR video traffic, the piecewise-constant-rate transmission and transport (PCRTT) method was used to optimize certain objectives while preserving continuous video playout. In [19], Liew and Chan developed bandwidth allocation schemes for multiple VBR videos to share a CBR channel. In [20], Salehi *et al.* presented an optimal algorithm for smoothing VBR video over a CBR link. Feng and Liu [21] introduced a critical bandwidth allocation algorithm to reduce the number of bandwidth variations and to maximize receiver buffer utilization. Because of the fundamental difference between wireless and wired links, these techniques cannot be directly applied to the problem of VBR video over wireless networks.

The downlink power allocation problem was studied in [23,24], aiming to obtain the power allocation that maximizes a properly defined system utility. A distributed algorithm based on dynamic pricing and partial cooperation was proposed. Deng, Webera, and Ahrens [32] studied the achievable maximum sum rate of multiuser interference channels. These papers provide the theoretical foundation and effective algorithms for utility maximization of downlink traffic, but the techniques used cannot be directly applied for VBR video over wireless networks with buffer and delay constraints.

In [33,34], the authors studied the problem of one VBR stream over a given time-varying wireless channel. In [33], it was shown that the separation between a delay jitter buffer and a decoder buffer is in general suboptimal, and several critical system parameters were derived. In [34], the authors studied the frequency of jitters under both network and video system constraint and provided a framework for quantifying the trade-offs among several system parameters.

In this paper, we jointly consider power control in wireless networks, playout buffers, and video frame information, address the more challenging problem of streaming multiple VBR videos, and present a cross-layer optimization approach that does not depend on any specific channel or video traffic models.

6. CONCLUSION

We developed a downlink power allocation model for streaming multiuser VBR videos in a cellular network. The model considers interactions among downlink power control, channel interference, playout buffers, and VBR video traffic characteristics. The formulated problem aims at maximizing the total transmission rate under both peak power and playout buffer overflow/underflow constraints. We presented a two-step approach for solving the problem and a distributed algorithm based on the dual decomposition technique. Our simulation studies validated the efficacy of the proposed algorithms.

ACKNOWLEDGEMENTS

This work is supported in part by the US National Science Foundation (NSF) under Grants CNS-0953513 and IIP-1127952 and through the NSF Wireless Internet Center for Advanced Technology at Auburn University. Any opinions, findings, and conclusions or recommendations expressed in this material are those of the author(s) and do not necessarily reflect the views of the foundation.

REFERENCES

- Huang Y, Mao S, Li Y. Downlink power allocation for stored variable-bit-rate videos. In *Proc. ICST QShine'10*, Houston, TX, Nov. 2010.
- Cisco. Cisco visual networking index: global mobile data traffic forecast update, 2010–2015. Feb. 2010, [online]. Available: http://www.cisco.com/en/US/solutions/collateral/ns341/ns525/ns537/ns705/ns827/white_paper_c11-520862.html
- Mao S, Lin S, Wang Y, Panwar S, Li Y. Multipath video transport over wireless ad hoc networks. *IEEE Wireless Communications* 2005; **12**(4):42–49.
- Kompella S, Mao S, Hou Y, Sherali H. Cross-layer optimized multipath routing for video communications in wireless networks. *IEEE Journal on Selected Areas in Communications* 2007; **25**(4):831–840.
- Kompella S, Mao S, Hou Y, Sherali H. On path selection and rate allocation for video in wireless mesh networks. *IEEE/ACM Transactions on Network* 2009; **17**(1):212–224.
- Chen M, Leung VC, Mao S. Directional controlled fusion in wireless sensor networks. *ACM/Springer Mobile Networks and Applications Journal* 2009; **14**(2):220–229.
- Soro S, Heinzelman W. A survey of visual sensor networks. *Advances in Multimedia* 2009; **2009** article ID 640386. doi:10.1155/2009/640386.
- Seema A, Reisslein M. Towards efficient wireless video sensor networks: a survey of existing node architectures and proposal for a Flexi-WVSNP design. *IEEE Communications Surveys and Tutorials* 2011; **13**(3):462–486.
- Zhao Y, Mao S, Neel J, Reed JH. Performance evaluation of cognitive radios: metrics, utility functions, and methodologies. *Proceedings of the IEEE* 2009; **97**(4):642–659.
- Hu D, Mao S, Hou YT, Reed JH. Fine grained scalability video multicast in cognitive radio networks. *IEEE Journal on Selected Areas in Communications* 2010; **28**(3):334–344.
- Hu D, Mao S. Streaming scalable videos over multi-hop cognitive radio networks. *IEEE Transactions on Wireless Communications* 2010; **9**(11):3501–3511.
- Hu D, Mao S, Reed JH. On video multicast in cognitive radio networks. In *Proc. IEEE INFOCOM 2009*, Rio de Janeiro, Brazil, Apr. 2009; 2222–2230.
- Hu D, Mao S. On medium grain scalable video streaming over cognitive radio femtocell networks. *IEEE Journal on Selected Areas in Communications* 2012; **30**:4.
- Hu D, Mao S. Resource allocation for medium grain scalable videos over femtocell cognitive radio networks. In *Proc. IEEE ICDCS 2011*, Minneapolis, MN, June 2011; 258–267.
- Hu D, Mao S. Cooperative relay with interference alignment for video over cognitive radio networks. In *Proc. IEEE INFOCOM 2012*, Orlando, FL, Mar. 2012.
- Alay O, Liu P, Guo Z, et al. Cooperative layered video multicast using randomized distributed space time codes. In *Proc. IEEE INFOCOM Workshops 2009*, Rio de Janeiro, Brazil, Apr. 2009; 1–6.
- Sistek H. Green-tech base stations cut diesel usage by 80 percent. CNET News, 2008.
- Lakshman T, Ortega A, Reibman A. VBR video: trade-offs and potentials. *Proceedings of the IEEE* 1998; **86**(1):952–973.
- Liew S, Chan H. Lossless aggregation: a scheme for transmitting multiple stored VBR video streams over a shared communications channel without loss of image quality. *IEEE Journal on Selected Areas in Communications* 1997; **15**(6):1181–1189.
- Salehi J, Zhang Z-L, Kurose J, Towsley D. Supporting stored video: reducing rate variability and end-to-end resource requirements through optimal smoothing. *IEEE/ACM Transactions on Networking* 1998; **6**(4):397–410.
- Feng W-C, Liu M. Critical bandwidth allocation techniques for stored video delivery across best-effort networks. In *Proc. IEEE ICDCS'00*, Taipei, Taiwan, Apr. 2000; 56–63.
- Chen M, Zakhor A. Multiple TFRC connections based rate control for wireless networks. *IEEE Transactions on Multimedia* 2006; **8**(5):1045–1062.
- Lee J, Mazumdar R, Shroff N. Downlink power allocation for multi-class wireless systems. *IEEE/ACM Transactions on Networking* 2005; **13**(4):854–867.
- Lee J, Kwon J. Utility-based power allocation for multiclass wireless systems. *IEEE Transactions on Vehicular Technology* 2009; **58**(7):3813–3819.
- Chiang M. Balancing transport and physical layers in wireless multihop networks: jointly optimal congestion control and power control. *IEEE Journal on Selected Areas in Communications* 2005; **23**(1):104–116.
- Gjendemsj A, Gesbert D, Oien G, Kiani S. Binary power control for sum rate maximization over multiple interfering links. *IEEE Transactions on Wireless Communications* 2008; **7**(8):3164–3173.

27. Mitra D. An asynchronous distributed algorithm for power control in cellular radio system. In *Proc. WINLAB Workshop on 3G Wireless Information Networks*, New Brunswick, NJ, Oct. 1993; 249–257.
28. Bertsekas D. *Nonlinear Programming*. Athena Scientific: Belmont, MA, 1995.
29. Palomar DP, Chiang M. A tutorial on decomposition methods for network utility maximization. *IEEE Journal on Selected Areas in Communications* 2006; **24**(8):1439–1451.
30. Reisslein M. Video trace library. Arizona State University, [online]. 2012. Available: <http://trace.eas.asu.edu/>
31. UMTS World. UMTS Power Control. [online]. 2012. Available: <http://www.umtsworld.com/technology/power.htm>
32. Deng S, Webera T, Ahrens A. Capacity optimizing power allocation in interference channels. *AEU International Journal of Electronics and Communications* 2009; **63**(2):139–147.
33. Stockhammer T, Jenkac H, Kuhn G. Streaming video over variable bit-rate wireless channels. *IEEE Transactions on Multimedia* 2004; **6**(2):268–277.
34. Liang G, Liang B. Balancing interruption frequency and buffering penalties in VBR video streaming. In *Proc. IEEE INFOCOM'07*, Anchorage, AK, May 2007; 1406–1414.